Journal of Macromolecular Science, Part A
Publication details, including instructions for authors and subscription information:
http://www.informaworld.com/smpp/title~content=t713597274

Polydispersity Effects on the Demixing Behavior of Poly(Vinyl Methyl Ether)/Polystyrene Blends

Margit T. Rätzsch[a]; Horst Kehlen[a]; Christian Wohlfarth[a]
[a] Chemistry Department, "Carl Schorlemmer" Technical University, Merseburg, German Democratic Republic

To cite this Article Rätzsch, Margit T. , Kehlen, Horst and Wohlfarth, Christian(1988) 'Polydispersity Effects on the Demixing Behavior of Poly(Vinyl Methyl Ether)/Polystyrene Blends', Journal of Macromolecular Science, Part A, 25: 9, 1055 — 1069
To link to this Article: DOI: 10.1080/00222338808053407
URL: http://dx.doi.org/10.1080/00222338808053407

J. MACROMOL. SCI.—CHEM., A25(9), pp. 1055-1069 (1988)

POLYDISPERSITY EFFECTS ON THE DEMIXING BEHAVIOR OF POLY(VINYL METHYL ETHER)/POLYSTYRENE BLENDS

MARGIT T. RÄTZSCH, HORST KEHLEN, and CHRISTIAN WOHLFARTH

Chemistry Department
"Carl Schorlemmer" Technical University
DDR-4200 Merseburg, German Democratic Republic

ABSTRACT

Phase equilibrium calculations for solutions or mixtures of synthetic polymers become considerably more difficult when there is polydispersity of the polymers. To simplify the calculations, polydispersity is often neglected in the calculations or accounted for in a summary way only, and often only relatively simple free energy relations are applied. For example, Halary et al. published experimental demixing data on poly(vinyl methyl ether)/polystyrene blends. In evaluating the data the following assumptions were made: 1) the minimum of the demixing curve equals the critical point, 2) the χ-parameter is independent of concentration and molecular weight, 3) the polydispersity may be roughly taken into account by using the formulas for monodisperse polymers and using the weight-average molecular weight. Continuous thermodynamics proves to be a suitable method to overcome the difficulties caused by polydispersity. Therefore, this method permits one to obtain detailed information on the phase equilibria in polymer solutions and in polymer blends in a relatively easy way. To show this, the data of Halary et al. are reanalyzed by means of continuous thermodynamics. In this way, more profound knowledge may be obtained from the experimental material, e.g., a more precise determination of the critical point and a more correct location of the spinodal.

INTRODUCTION

The poly(vinyl methyl ether)/polystyrene blend (PVME + PS) can be considered today as a standard system for the investigation of polymer compatibility in the melt [1-15], comparable to solutions of polystyrene in cyclohexane for the case of liquid-liquid equilibrium in polymer solutions. On the one hand, this is due to the good availability of well-characterized polystyrene samples of any desired molecular weight (MW). On the other hand, the technique of static quenching of fluorescence emission offers a very convenient way for the precise investigation of the demixing region in these blends by use of anthracene-labeled polystyrenes. The appearance of phase separation is characterized by sharp cessation of fluorescence quenching, and equilibrium, as well as kinetic, effects may be studied [1-4, 13-15].

In 1986, Halary et al. published a systematic series of demixing curves and spinodals for this blend [1, 2], covering a very broad range of mean MW and establishing a well-documented effect of mean MW. In their thermodynamic analysis of the primary data, they neglected the effect of polydispersity and considered the minimum of the demixing curve to be the critical point. This cannot be correct because poly(vinyl methyl ether) samples are characterized by rather broad MW distributions (MWD). The minimum of the demixing curve and the critical point in polydisperse systems do not coincide. The spinodal and the demixing curve possess a common tangent at the critical point, which has a nonzero slope. The minima of both curves differ in concentration and temperature. Within their discussion of the effect of mean molar mass, Halary et al. found a correlation between the minimum of the demixing curve and the weight-average MW in the form $\psi_{PS}^{-1} = 1 + k\bar{M}_{w,PS}^{1/2}$ [2]. This fact is usually interpreted as a polydispersity effect, but it is not a sufficient proof of the assumption that this minimum is equal to the critical point. Since the work of Koningsveld on polydisperse polymer solutions [16], it is well-known that the threshold temperature (i.e., the extremum) behaves in a manner analogous to the critical point if type and principal shape of the MWD do not change within a series as will be the case here.

Continuous thermodynamics permits a complete and correct treatment of polydispersity effects on polymer compatibility [17-19]. The aim of this paper is to reanalyze the data of Halary et al. [1, 2] to account for the true effect of MWD by continuous thermodynamics. In this way, consistent information on the demixing curve (cloud-point curve) and the related shadow curve, the critical point, and the spinodal will be provided, thereby giving deeper insight into the compatibility behavior of the blend.

BASIC EQUATIONS

Polystyrene and poly(vinyl methyl ether) samples can be characterized by the Schulz-Flory distribution function, reading for a Polymer B:

$$W_B(r) = \frac{k_B{}^{k_B+1}}{\bar{r}_{n,B}\Gamma(k_B+1)} \left(\frac{r}{\bar{r}_{n,B}}\right)^{k_B} \exp\left(-k_B \frac{r}{\bar{r}_{n,B}}\right), \tag{1}$$

where r is the number of segments for the considered polymer species and $\bar{r}_{n,B}$ is the corresponding number average. Γ means the gamma-function. The parameter k_B is related to mass (weight) and the number average of r by

$$k_B = 1/(\bar{r}_{w,B}/\bar{r}_{n,B} - 1).$$

The demixing curves given by Halary et al. [1, 2] describe the temperature at the beginning of the phase separation process as a function of the composition $\psi_B{}'$ of the phase $'$ with given Polymers B (PVME) and C (PS) characterized by their distribution functions $W_B(r)$ and $W_C(r)$. For multicomponent systems, such a curve is usually called a cloud-point curve. The related shadow curve then provides the composition $\psi_B{}''$ of the first droplets of the newly formed phase $''$. Both curves are identical for strictly binary mixtures but not for the polydisperse blend considered here. For such systems, continuous thermodynamics [17, 18] leads to a set of only three equations that provide all necessary information on the cloud point/shadow point problem:

$$\psi_B{}'' = \int \psi_B{}' W_B{}'(r) \exp(\rho_B r)\, dr \tag{2}$$

$$\psi_C{}'' = \int \psi_C{}' W_C{}'(r) \exp(\rho_C r)\, dr \tag{3}$$

$$\frac{1}{\bar{r}_n{}''} \equiv \frac{\psi_B{}''}{\bar{r}_{n,B}{}''} + \frac{\psi_C{}''}{\bar{r}_{n,C}{}''} = \int \psi_B{}' \frac{W_B{}'(r)}{r} \exp(\rho_B r)\, dr + \int \psi_C{}' \frac{W_C{}'(r)}{r} \exp(\rho_C r)\, dr. \tag{4}$$

Segments of both Polymers B and C are chosen to be of equal size, and $\bar{r}_n$ is the number-average segment number for the total phase considered.

Integration obeys the normalization condition for the distribution function:

$$\int W(r)\,dr = 1. \tag{5}$$

All integrals are to be taken over the total r-intervals occurring. ψ_B is the overall segment fraction of the Polymer B in a phase where

$$\psi_B{}^{\alpha} + \psi_C{}^{\alpha} = 1 \quad \text{with} \quad \alpha = ' \text{ or } ''. \tag{6}$$

The quantities of ρ_B and ρ_C are defined by

$$\rho_K = \frac{1}{\bar{r}_n''} - \frac{1}{\bar{r}_n'} - \ln \bar{\bar{\gamma}}_K'' + \ln \bar{\bar{\gamma}}_K' \quad \text{with} \quad K = B, C. \tag{7}$$

To calculate the segment molar activity coefficients $\bar{\bar{\gamma}}_K$, a $\bar{\bar{G}}^E$-model proposed by Tompa [20] is assumed to be sufficient for the title blend [18]:

$$\frac{\bar{\bar{G}}^E}{RT} = \psi_B(1 - \psi_B)(1 + c\psi_B + d\psi_B{}^2)\,\beta(T). \tag{8}$$

$\bar{\bar{G}}^E$ is the deviation of Gibbs free energy from its value for a Flory-Huggins mixture (with $\chi = 0$) considered for a mole of segments [21], R is the gas constant, and T is the absolute temperature. The function $\beta(T)$ represents the temperature dependence of $\bar{\bar{G}}^E/RT$ (in analogy to the simple χ-function). An analytical expression for $\beta(T)$ does not need to be specified here. $\bar{\bar{\gamma}}_K$ is obtained from Eq. (8), reading [17]

$$\ln \bar{\bar{\gamma}}_B = (1 - \psi_B)^2\ [1 + 2c\psi_B + 3d\psi_B{}^2]\,\beta(T), \tag{9}$$

$$\ln \bar{\bar{\gamma}}_C = \psi_B{}^2\ [1 - c + 2(c - d)\psi_B + 3d\psi_B{}^2]\,\beta(T). \tag{10}$$

$\bar{\bar{G}}^E$ and $\bar{\bar{\gamma}}_K$ contain two adjustable parameters, c and d (Halary et al. [2] assumed $c = d = 0$). Some experimental cloud points or the critical point are usually chosen for fitting these parameters.

ANALYTIC INTEGRABILITY

For the case of the Schulz-Flory distribution functions, all integrations in Eqs. (2)-(4) can be performed analytically, leading to

$$\psi_B'' = \psi_B'/(1 - \bar{r}_{n,B}'\rho_B/k_B)^{k_B+1} \tag{11}$$

and

$$\bar{r}_{n,B}'' = \bar{r}_{n,B}'/(1 - \bar{r}_{n,B}'\rho_B/k_B), \tag{12}$$

and corresponding equations for ψ_C'' and $\bar{r}_{n,C}''$ obtained from Eqs. (11) and (12) by substituting C for B. After rearrangement of Eqs. (11) and (12) we get

$$\rho_K = \left[1 - \left(\frac{\psi_K'}{\psi_K''}\right)^{1/(k_K+1)}\right] \frac{k_K}{\bar{r}_{n,K}'} \quad \text{with } K = B, C. \tag{13}$$

Using Eqs. (7), (9), and (10), we find

$$\rho_C - \rho_B = \beta(T)Z, \tag{14}$$

$$Z = 2(1 - c)(\psi_B' - \psi_B'') + 3(c - d)(\psi_B'^2 - \psi_B''^2) + 4d(\psi_B'^3 - \psi_B''^3), \tag{15}$$

$$\ln(\bar{\bar{\gamma}}_C'/\bar{\bar{\gamma}}_C'') = \beta(T)Y, \tag{16}$$

$$Y = (1 - c)(\psi_B'^2 - \psi_B''^2) + 2(c - d)(\psi_B'^3 - \psi_B''^3) + 3d(\psi_B'^4 - \psi_B''^4). \tag{17}$$

Equations (4) and (11)-(17) permit the elimination of all other variables, resulting in a single equation for the unknown ψ_B'':

$$F \equiv -\rho_B\,\psi_B'/k_B - \rho_C(1 + (1 - \psi_B'')/k_C) + (\psi_B'' - \psi_B')\,(1/\bar{r}_{n,B}' - 1/\bar{r}_{n,B}'') + Y(\rho_C - \rho_B)/Z = 0, \tag{18}$$

which can be solved numerically by Newton's method. In Eq. (18), ρ_B and ρ_C are given by Eq. (13). Hence, continuous thermodynamics provides an enormous reduction in the computational burden of calculating cloud-point curves and shadow curves, especially in the case of Schulz-Flory distributions.

SPINODAL CURVE AND CRITICAL POINT

The equations for spinodal curve and critical point are derived from the stability conditions [22, 23].

Spinodal curve:

$$\frac{1}{\psi_B \bar{r}_{w,B}} + \frac{1}{\psi_C \bar{r}_{w,C}} + 2\beta(T)[c - 1 + 3(d - c)\psi_B - 6d\psi_B{}^2] = 0. \tag{19}$$

Critical point:

$$-\frac{\bar{r}_{z,B}}{\psi_B{}^2 \bar{r}_{w,B}{}^2} + \frac{\bar{r}_{z,C}}{\psi_C{}^2 \bar{r}_{w,C}{}^2} + 6\beta(T)[d - c - 4d\psi_B] = 0, \tag{20}$$

where the critical point also has to fulfill Eq. (19), and $\bar{r}_z$ means the z-average of r.

EXTREMUM OF THE CLOUD-POINT CURVE

Halary et al. [1, 2] represented all demixing curves in figures and only the minima in a table. Hence, the minimum is used for calculation of the parameters. If, according to earlier results [18], the simplification $d = 0$ is applied, this point is sufficient for calculation of the remaining parameter c.

The extremum condition of the cloud-point curve reads

$$\left(\frac{\partial T}{\partial \psi_B{}'}\right)_P = 0. \tag{21}$$

Considering the function $\beta(T)$ to be monotonous, Eq. (21) is equivalent to

$$\left(\frac{\partial \beta(T)}{\partial \psi_B{}'}\right)_P = 0,$$

and we do not need to differentiate the cloud-point equation implicitly with respect to T and $\psi_B{}'$ but can use Eq. (14):

$$\left(\frac{\partial[(\rho_C - \rho_B)/Z]}{\partial \psi_B{}'}\right)_P = 0. \tag{22}$$

This differentiation is straightforward. It needs only to be noted that $d\psi_B{}' = -d\psi_C{}'$ and that the partial derivative $(\partial \psi_B{}''/\partial \psi_B{}')_P$ may be calculated by implicit differentiation:

$$\left(\frac{\partial \psi_B''}{\partial \psi_B'}\right)_P = -\frac{(\partial F/\partial \psi_B')_{\psi_B'',P}}{(\partial F/\partial \psi_B'')_{\psi_B',P}}, \tag{23}$$

where F is given by Eq. (18).

The system of Eqs. (18) and (23) is solved with respect to the parameter c and the concentration ψ_B'' corresponding to the minimum of the shadow curve by using Powell's procedure.

Thus, by applying $d = 0$, we are able to calculate the complete cloud-point curve and the shadow curve together with the critical point and the spinodal curve on the basis of only the extremum value of the experimental demixing curve (i.e., the cloud-point curve).

As outlined below, it is desirable to also perform calculations maintaining the two parameters c and d. Then a further point of the cloud-point curve is used additionally for calculation of the parameters.

RESULTS AND DISCUSSION

The Schulz-Flory parameters for the polymer samples (nomenclature follows Refs. 1 and 2) and the result of the parameter estimation according to the procedure outlined above are summarized in Table 1. The index B in all equations given above corresponds to poly(vinyl methyl ether) and C to polystyrene. It is obvious that the assumption of Halary et al. [2] $-\chi$ being a constant parameter, i.e., $c = d = 0$—is a very crude one. Furthermore, a much larger variation of $\bar{\bar{G}}^E$ with the mean MW is observed than expected from our earlier results [18]. This indicates a more complex behavior of the Gibbs free energy function and of the binodal plane than that obtained by using only one parameter. Nevertheless, the main features can be discussed on this basis.

Table 2 lists the minima of the cloud-point curves measured by Halary et al. [1, 2], the calculated minima of the shadow curves, and the calculated critical points for all blends. To show the differences clearly, the calculated results are given for three figures in all cases. The distances between both minima and between them and the critical solution point are appreciable and cannot be neglected, as Halary et al. assumed. Figure 1 presents the complete calculated curves for two examples (a blend with low mean MW's and a blend with high ones), where $1/\beta(T)$ is used as a measure of temperature.

The figure shows clearly that the location of the spinodal curve is also unprecise in the papers of Halary et al. [1, 2]. The minima of the cloud-point

TABLE 1. Parameters of the Schulz-Flory Distributions Characterizing the Polymers and Parameters of the $\bar{\bar{G}}^E$ Model Applied[a]

Blend[b]	$\bar{M}_{n,\mathrm{PVME}}$	k_{PVME}	$\bar{M}_{n,\mathrm{PS}}$	k_{PS}	One-parameter version ($d = 0$), c	Two-parameter version	
						c	d
V99-S20	46 500	0.893	19 300	16.67	0.530	0.5204	0.008
V99-S35	46 500	0.893	34 000	20.0	0.575	0.5697	0.004
V99-S67	46 500	0.893	62 000	12.5	2.003	-0.6825	0.732
V99-S106	46 500	0.893	100 000	16.67	3.249	-0.3515	0.630
V99-S233	46 500	0.893	220 000	16.67	3.563	-0.2093	0.528
V99-S381	46 500	0.893	307 000	4.17	4.214	-0.0541	0.662
V99-S600	46 500	0.893	545 000	10.0	4.638	-0.0097	0.446
V99-S759	46 500	0.893	660 000	6.67	5.466	0.0339	0.443
V99-S1660	46 500	0.893	1 330 000	3.57	2.938	0.0106	0.346
V45-S106	22 000	0.952	100 000	16.67	1.385	-0.1918	0.401
V388-S106	229 000	1.45	100 000	16.67	0.161	0.1632	-0.003
V633-S106	370 000	1.41	100 000	16.67	0.169	0.1666	0.000
V1330-S106	547 000	0.680	100 000	16.67	0.205	0.2058	0.000
V388-S233	229 000	1.45	220 000	16.67	0.950	0.7196	0.101
V388-S600	229 000	1.45	545 000	10.0	1.045	-0.0300	0.354

[a]Index B corresponds to PVME and C to PS.
[b]Nomenclature corresponding to Ref. 2: V = poly(vinyl methyl ether), PVME; S = polystyrene, PS.

TABLE 2. Weight Fractions of Polystyrene at the Minima of the Cloud-Point Curve and of the Shadow Curve, and at the Critical Point

Blend[a]	Minimum of cloud-point curve	Minimum of shadow curve	Critical point
V99-S20	0.55	0.439	0.515
V99-S35	0.50	0.383	0.460
V99-S67	0.29	0.336	0.333
V99-S106	0.235	0.293	0.289
V99-S233	0.175	0.252	0.240
V99-S381	0.125	0.225	0.205
V99-S600	0.12	0.195	0.182
V99-S759	0.11	0.182	0.170
V99-S1660	0.08	0.146	0.136
V45-S106	0.20	0.269	0.248
V388-S106	0.67	0.491	0.573
V638-S106	0.72	0.544	0.625
V1330-S106	0.80	0.587	0.680
V388-S233	0.40	0.328	0.368
V388-S600	0.30	0.286	0.296

[a]See Table 1, Footnote b.

curve and the spinodal do not coincide, but both curves are tangent to each other at the critical point. The spinodal minimum is situated at a slightly higher temperature than that of the cloud-point curve. Therefore, the further assumption of Halary et al. [2] that the difference in ΔT between the cloud-point curve and the spinodal is independent of the blend composition is incorrect. As their experiments do not allow verification of this assumption, there should be some doubt about this method of obtaining spinodal data.

Figure 2 shows the minima of the cloud-point curves, the minima of the

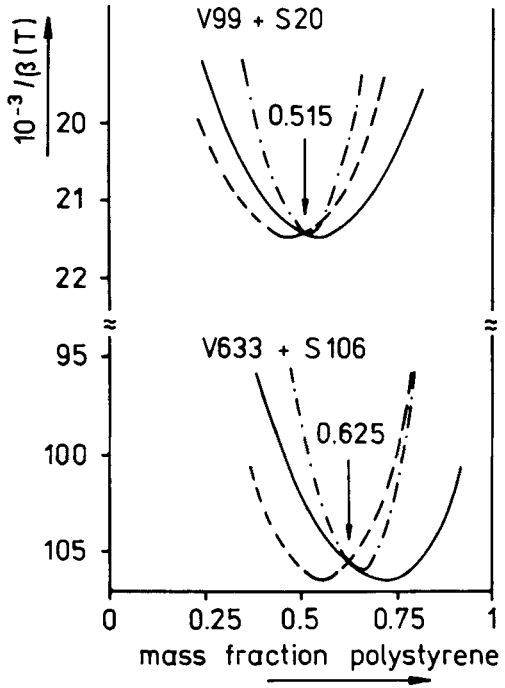

FIG. 1. Examples for calculated cloud-point curves (—), shadow curves (---), and spinodals (– • –). The arrows point to the critical concentration. The function $1/\beta(T)$ is used as a measure of temperature.

shadow curves, and the critical points for a number of blends, keeping one component constant in each case. Figure 2(a) corresponds to Fig. 4 in Ref. 2 (where the differences between these three curves are neglected). Figure 2 indicates that this neglect leads to a rather rough approximation.

Furthermore, Fig. 2 exhibits an interesting feature: the three curves intersect at a special point. At this point, but only at this point, the minimum of the cloud-point curve, the minimum of the shadow curve, and the critical point coincide. The interpolated values of the mean MW at this intersection point are $\bar{M}_{w,\mathrm{PS}} \approx 69\,300$ for V99 + PS and $\bar{M}_{w,\mathrm{PVME}} \approx 113\,400$ for PVME + S106.

Figure 3 presents two diagrams showing $1/\psi_{\mathrm{PS}}$ versus $(\bar{r}_{w,\mathrm{PS}}/\bar{r}_{w,\mathrm{PVME}})^{1/2}$ for the minima of the cloud-point curves, the minima of the shadow curves,

and the critical points. The same systems as in Fig. 2 were chosen, i.e., one mixing partner is kept constant in each case. Figure 3(a) is similar to Fig. 9 in Ref. 2 where no distinction is made between the three curves. As the theoretical basis for the approximately linear dependence, Halary et al. quote the relation (written in our notation)

$$1/\psi_{PS} = 1 + (r_{PS}/r_{PVME})^{1/2}, \tag{24}$$

where the segment numbers, r_{PS} and r_{PVME}, are replaced by the corresponding weight averages, $\bar{r}_{w,PS}$ and $\bar{r}_{w,PVME}$, respectively. However, the experimental data usually do not correspond to this relation. Hence, Halary et al., following Nishi's earlier work [24, 25], introduced a fitting factor α,

$$1/\psi_{PS} = 1 + \alpha(r_{PS}/r_{PVME})^{1/2}, \tag{25}$$

which is significantly larger than unity in many cases (Table III in Ref. 2).

However, Eq. (24) results from Eq. (20) by applying $c = d = 0$ (corresponding to a χ-value independent of composition) and neglecting polydispersity ($\bar{r}_w = \bar{r}_z$). The values of Table 1 show the approximation $c = d = 0$ to be unsatisfactory. If, nevertheless, this approximation is made, Eq. (20) results in

$$1/\psi_{PS} = 1 + \frac{\bar{r}_{w,PS}/\bar{r}_{z,PS}^{1/2}}{\bar{r}_{w,PVME}/\bar{r}_{z,PVME}^{1/2}} = 1 + \left(\frac{\bar{r}_{w,PS}}{\bar{r}_{w,PVME}}\right)^{1/2} \left[\frac{k_{PS}+1}{k_{PS}+2}\,\frac{k_{PVME}+1}{k_{PVME}+2}\right]^{1/2} \tag{26}$$

Hence, the polydispersity is not sufficiently accounted for by replacing the segment numbers in the formula for the monodisperse case, Eq. (24), by the corresponding weight averages.

The most important point, however, is that, in discussing Eqs. (24) and (26), the critical points have to be used instead of the minimum data. Considering the minima of the cloud-point curves, it can be seen from Fig. 3 that the mean slope of the plot of $1/\psi_{PS}$ versus $(\bar{r}_{w,PS}/\bar{r}_{w,PVME})^{1/2}$ equals approximately 3.1 for systems V99 + polystyrene and approximately 2.7 for systems poly(vinyl methyl ether) + S106. The slope reduces to 1.6 and 2.2, respectively, if the critical data are considered. Therefore, the conclusions of Halary et al. [2] regarding a much too large effective segment length of poly(vinyl methyl ether) in these blends are not necessary.

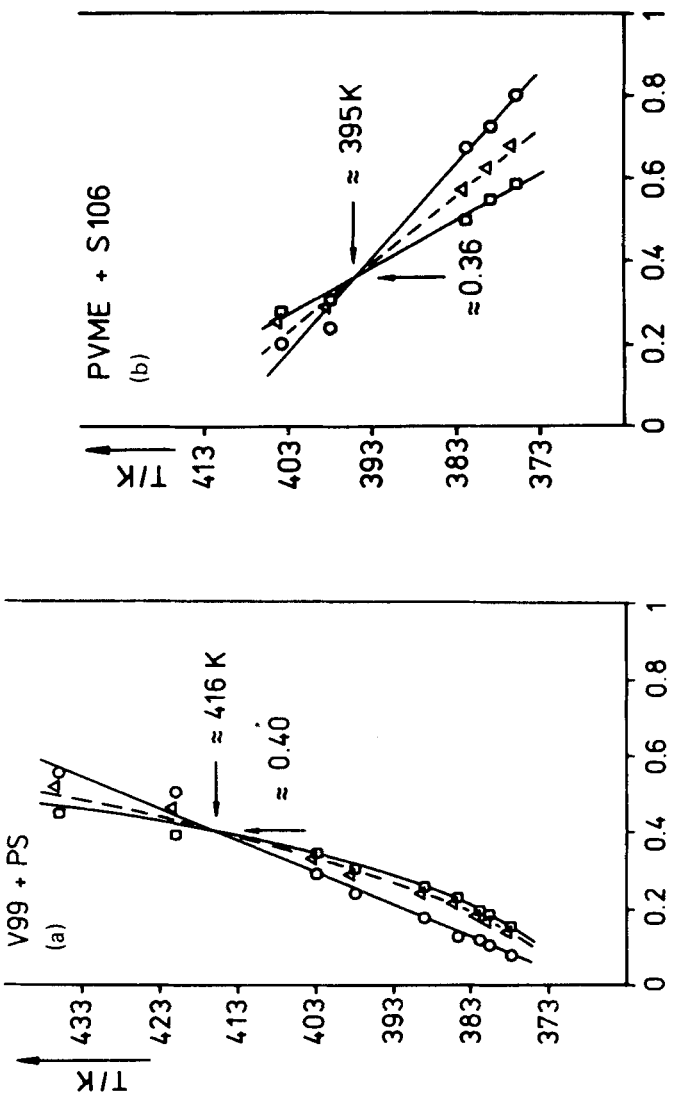

FIG. 2. Plot of temperature vs composition showing the experimental minima of the cloud-point curves (○), the calculated minima of the shadow curves (□), and the calculated critical points (△). Lines are hand drawn. (a) V99 + different polystyrenes. (b) Different poly(vinyl methyl ether)s + S106.

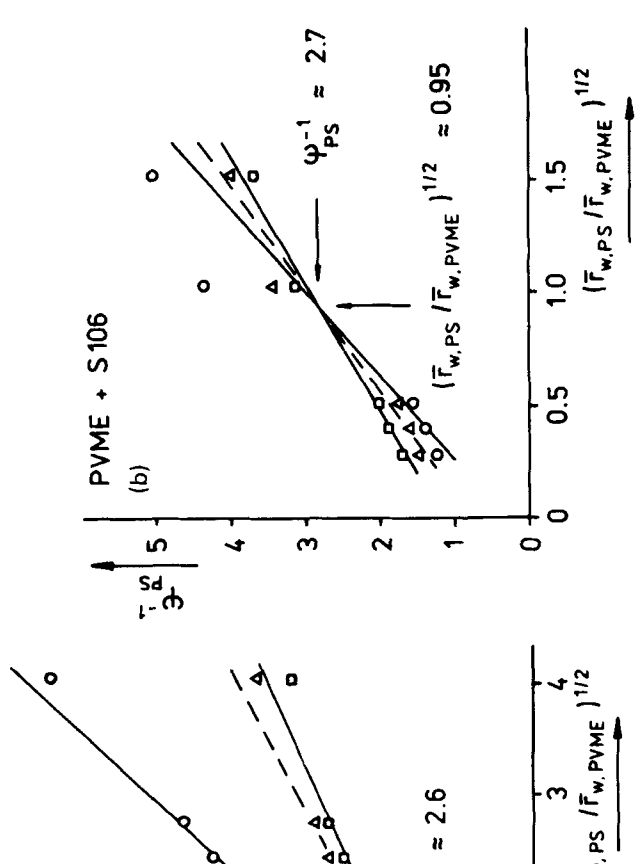

FIG. 3. Plot of the reciprocal of the polystyrene segment fraction, $1/\psi_{PS}$, vs the square root of the quotient of the weight-average segment numbers, $(\bar{r}_{w,PS}/\bar{r}_{w,PVME})^{1/2}$, showing the experimental minima of the cloud-point curves (○), the calculated minima of the shadow curves (□), and the calculated critical points (△). Lines are hand drawn. (a) V99 + different polystyrenes. (b) Different poly(vinyl methyl ether)s + S106.

All deviations from the simple Eq. (24) can be explained by the two main effects on the phase diagram in polymer blends: the free energy relation and the polydispersity described by the distribution function. Neither the application of a χ-parameter independent of the composition nor the neglect of the polydispersity (identification of the cloud-point curve minimum with the critical point and of $\bar{r}_z$ with $\bar{r}_w$) are valid in the analysis of the considered blends.

More information could be obtained if all data would be available in numerical form. Because only one parameter can be fitted to the minimum of the cloud-point curves, we were forced to use a one-parameter $\bar{\bar{G}}^E$ model. Table 1 shows the limitations of this procedure. The one-parameter model leads to c values being unsatisfyingly large for some blends. We tried to improve this situation by adjusting the parameter d to a further point of the cloud-point curve taken from the corresponding figure [1, 2]. The critical composition obtained in this way is practically unchanged and so are all qualitative discussions given above. A definite dependence of the parameter c on the mean MW is observed, which requires a $\bar{\bar{G}}^E$ function depending on the moments of the distribution function. Such an analysis needs more extended and complete experimental material.

CONCLUSIONS

To overcome the difficulties connected with the polydispersity of polymers, simplifying assumptions, similar to those in the papers by Halary et al., are often made in the literature on phase equilibria of polymers. The present paper shows that these simplifying assumptions are unnecessary. Continuous thermodynamics proves to be a convenient tool for evaluating the existing experimental data without simplifying assumptions and without large computational efforts.

REFERENCES

[1] J. L. Halary, J. M. Ubrich, J. M. Nunzi, L. Monnerie, and R. S. Stein, *Polymer, 25,* 956 (1984).

[2] J. M. Ubrich, F. Ben Cheikh Larbi, J. L. Halary, L. Monnerie, B. J. Bauer, and C. C. Han, *Macromolecules, 19,* 810 (1986).

[3] J. L. Halary, J. M. Ubrich, L. Monnerie, H. Yang, and R. S. Stein, *Polym. Commun., 26,* 73 (1985).

[4] F. Ben Cheikh Larbi, S. Lelong, J. L. Halary, and L. Monnerie, *Ibid., 27,* 23 (1986).
[5] M. Bank, J. Leffingwell, and C. J. Thies, *J. Polym. Sci., Part A-2, 10,* 1097 (1972).
[6] T. Nishi, T. T. Wang, and T. K. Kwei, *Macromolecules, 8,* 227 (1975).
[7] H. L. Snyder and P. Meakin, *Polym. Prepr., 24,* 411 (1983).
[8] L. P. McMaster, *Ibid., 6,* 760 (1973).
[9] H. Yang, G. Hadziionnou, and R. S. Stein, *J. Polym. Sci., Polym. Phys. Ed., 21,* 159 (1983).
[10] H. Yang, M. Shibayama, R. S. Stein, and C. C. Han, *Polym. Bull., 12,* 7 (1984).
[11] M. Irie and R. Iga, *Makromol. Chem., Rapid Commun., 7,* 751 (1986).
[12] T. Nishi and T. K. Kwei, *Polymer, 16,* 285 (1975).
[13] C. C. Han, M. Okada, Y. Muroga, F. L. McCrackin, B. J. Bauer, and Q. Tran-Cong, *Polym. Eng. Sci., 26,* 3 (1986).
[14] C. W. Frank, *Report ARO-18453,5-CH,* Stanford University, 1986; *Chem. Abstr., 106,* 19312g.
[15] H. Yang, M. Shibayama, R. S. Stein, N. Shimizu, and T. Hashimoto, *Macromolecules, 19,* 1667 (1986).
[16] R. Koningsveld, in *Polymer Science* (A. D. Jenkins, ed.), North-Holland, Amsterdam, 1972, p. 1065 ff.
[17] H. Kehlen and M. T. Rätzsch, *Z. Phys. Chem. (Leipzig), 264,* 1153 (1983).
[18] M. T. Rätzsch, H. Kehlen, and D. Thieme, *J. Macromol. Sci.–Chem., A23,* 811 (1986).
[19] M. T. Rätzsch, H. Kehlen, and D. Thieme, *Ibid., A24,* 991 (1987).
[20] H. Tompa, *Polymer Solutions,* Butterworths, London, 1956.
[21] M. T. Rätzsch and Ch. Wohlfarth, *Wiss, Z. Tech. Hochsch. Leuna-Merseburg, 24,* 415 (1982).
[22] S. Beerbaum, J. Bergmann, H. Kehlen, and M. T. Rätzsch, *Proc. R. Soc. London, A406,* 63 (1986).
[23] H. Kehlen, M. T. Rätzsch, and J. Bergmann, *J. Macromol. Sci.–Chem., A24,* 1 (1987).
[24] T. Nishi, *Rep. Prog. Polym. Phys. Jpn., 20,* 225 (1977).
[25] T. Nishi, *J. Macromol. Sci.–Phys., B17,* 517 (1980).

Received July 3, 1987
Revision received February 1, 1988